Published in final edited form as:
Chem Res Toxicol. 2013 November 18; 26(11): . doi:10.1021/tx400229e.

OXIDATION OF POLYCHLORINATED BIPHENYLS BY LIVER TISSUE SLICES FROM PHENOBARBITAL-PRETREATED MICE IS CONGENER-SPECIFIC AND ATROPSELECTIVE

Xianai Wu[a], **Michael Duffel**[b], and **Hans-Joachim Lehmler**[a]

[a]Department of Occupational and Environmental Health, College of Public Health, The University of Iowa, Iowa City, IA 52242

[b]Department of Pharmaceutical Sciences and Experimental Therapeutics, College of Pharmacy, The University of Iowa, Iowa City, IA 52242

Abstract

Mouse models are powerful tools to study the developmental neurotoxicity of polychlorinated biphenyls (PCBs); however, studies of the oxidation of chiral PCB congeners to potentially neurotoxic hydroxylated metabolites (OH-PCBs) in mice have not been reported. Here we investigate the atropselective oxidation of chiral PCB 91 (2,2',3,4',6-pentachlorobiphenyl), PCB 95 (2,2',3,5',6-pentachlorobiphenyl), PCB 132 (2,2',3,3',4,6'-hexachlorobiphenyl), PCB 136 (2,2',3,3',6,6'-hexachlorobiphenyl) and PCB 149 (2,2',3,4',5',6-hexachlorobiphenyl) to OH-PCBs in liver tissue slices prepared from female mice. The metabolite profile of PCB 136 typically followed the rank order 5-OH-PCB > 4-OH-PCB > 4,5-OH-PCB, and metabolite levels increased with PCB concentration and incubation time. A similar OH-PCB profile was observed with the other PCB congeners, with 5-OH-PCB:4-OH-PCB ratios ranging from 2 to 12. More 5-OH-PCB 136 was formed in liver tissue slices obtained from animals pretreated with phenobarbital (P450 2B inducer) or, to a lesser extent, dexamethasone (P450 2B and 3A enzyme inducer) compared to tissue slices prepared from vehicle-pretreated animals. The apparent rate of 5-OH-PCBs formation followed the approximate rank order PCB 149 > PCB 91 > PCB 132 ~ PCB 136 > PCB 95. Atropselective gas chromatography revealed a congener-specific atropisomeric enrichment of major OH-PCB metabolites. Comparison of our results with published OH-PCB patterns and chiral signatures (i.e., the direction and extent of the atropisomeric enrichment) from rat liver microsomal revealed drastic differences between both species, especially following induction of P450 2B enzymes. These species differences in the metabolism of chiral PCBs should be considered in developmental neurotoxicity studies of PCBs.

Keywords

Chirality; P450 enzymes; P450 2B enzymes; environmental pollutants; precision-cut tissue slices; enantioselective

Corresponding Author: Dr. Hans-Joachim Lehmler, The University of Iowa, Department of Occupational and Environmental Health, University of Iowa Research Park, #221 IREH, Iowa City, IA 52242-5000, Phone: (319) 335-4310, Fax: (319) 335-4290, hans-joachim-lehmler@uiowa.edu.

SUPPORTING INFORMATION AVAILABLE

The supporting information includes effect of PB, DEX and vehicle control-pretreatment on body and liver weights in female mice used for preparation of liver slices; limits of detection of PCBs and OH-PCBs; enantiomeric fraction values of racemic standards, resolution, temperature programs, and retention time of PCB and OH-PCB atropisomers in liver tissue slice incubations; protein, PCB and OH-PCB levels in liver tissue slices from PB-pretreated mice; representative GC-MS chromatograms confirming OH-PCB metabolites formed by mouse liver tissue slices; representative GC-ECD chromatograms illustrating the atropisomeric enrichment of OH-PCBs on different atropselective columns. This material is available free of charge via the Internet at http://pubs.acs.org.

INTRODUCTION

Neurodevelopmental disorders, such as learning disabilities, sensory deficits, developmental delays, and attention deficits, occur frequently in the human population and cause lifelong disabilities that are costly to families and society.[1] Although their origin is frequently unknown, a considerable percentage of neurodevelopmental disorders have been linked to exposure to environmental toxicants, including persistent organic pollutants (POPs).[2] Epidemiological and laboratory studies have demonstrated that chronic, low-level developmental exposure to PCBs, an important class of POPs, is related to neurological and behavioral disturbances in infants and children.[3, 4] In particular non-dioxin-like PCB congeners with *ortho* substituents have been linked to neurodevelopmental toxicity following exposure to PCBs. These PCB congeners do not bind to the aryl hydrocarbon receptor (AhR),[5] but cause AhR-independent effects on neurotransmitter functions in the central nervous system and alter processes related to calcium signaling.[6, 7] In particular ryanodine receptor (RyR) activation by multiple *ortho* substituted PCBs is a highly sensitive mechanism thought to play an important role in adverse neurodevelopmental effects following PCB exposure.[8] For example, the deficits in spatial learning and memory observed in weanling rats exposed to Aroclor 1254, a commercial PCB mixture rich in multiple *ortho* substituted PCBs, are likely linked to altered dendritic growth and plasticity following RyR activation by chiral PCBs.[9–11]

Several PCB congeners and their hydroxylated metabolites with three or four *ortho* chlorine substituents and an asymmetric substitution pattern on both phenyl rings are chiral. They exist as two stable rotational isomers, called atropisomers, which are non-superimposable mirror images of each other. Chiral PCB congeners are major, RyR-active components of technical PCB mixtures.[12, 13] They are present as a racemate (a 1:1 ratio of both atropisomers) in commercial products, but can display atropisomeric enrichment (i.e., a shift in the ratio of both atropisomers) in wildlife, laboratory animals and humans.[14] *In vitro* studies have shown that PCB 136, a chiral PCB congener, causes RyR activation in an atropisomer-specific manner.[15] PCB 84 atropisomers atropselectively affected [^{3}H] phorbol ester binding in rat cerebellar granule cells and $^{45}Ca^{2+}$-uptake in rat cerebellum, two other modes of action implicated in PCB neurodevelopmental toxicity.[16] Thus, the extent of the atropisomeric enrichment of chiral PCBs may play a role in their neurodevelopmental toxicity. Analogous to the parent PCBs, OH-PCBs may also adversely affect neurodevelopment in humans,[17] possibly by altering processes related to calcium signaling[8, 18, 19] or thyroid function.[20] There is growing evidence that chiral OH-PCB metabolites undergo atropisomeric enrichment *in vivo*[21, 22] and, like their parent compounds, are transferred across the placenta.[23] Consequently, the profiles and chiral signatures of OH-PCBs may play a currently overlooked role in the neurodevelopmental toxicity of PCBs.

Metabolism studies with recombinant rat P450 2B1 and dog P450 2B11 enzymes,[24] rat and human liver microsomes,[25–27] and rat liver tissue slices[28] have shown that chiral PCBs with a 2,3,6-trichloro substitution pattern are metabolized to 4- and 5-OH-PCBs in mammals (Figure 1). Furthermore, the metabolism of chiral PCBs by rat and human P450 enzymes is atropselective, with P450 2B isoforms atropselectively metabolizing chiral PCBs to OH-PCB.[26–30] The observation that P450 2B enzymes metabolize chiral PCBs is important because developmental exposure to PCB mixtures increases hepatic gene expression and activities of P450 2B enzymes.[10, 11] The induction of P450 2B enzymes in dams in particular will facilitate the metabolism of chiral PCBs to potentially neurotoxic OH-PCBs.

Limited *in vivo* experiments also reveal atropisomeric enrichment of both the chiral parent PCB and the corresponding OH-PCB metabolites in mice and rats.[21, 22] The direction and extent of the atropisomeric enrichment of PCBs is species and congener-dependent. For example, rat P450 2B1, but not human P450 2B6, metabolizes PCB 91 atropselectively.[29] Similarly, (+)-PCB 136 displays considerable atropisomeric enrichment in mice,[31] while (−)-PCB is slightly enriched in rats.[22] Therefore, it is likely that there are species dependent differences in the atropselective formation of potentially neurotoxic OH-PCBs.

Mouse models are emerging as a powerful tool to study gene-environment interactions in human neurodevelopmental disorders[32, 33] and have been used to study the effect of PCBs on adverse developmental outcomes following PCB exposure.[34] Therefore, it is increasingly important to understand the metabolism and disposition of neurotoxic PCB congeners in mice. Unfortunately, studies of the atropselective formation OH-PCBs from neurotoxic PCB congeners in mice have not been reported previously, especially following induction of P450 2B enzymes. Therefore, the present study investigated the metabolism of environmentally relevant, RyR-active PCBs 91, 95, 132, 136 and 149 using liver tissue slices from adult female mice, with the goal of gaining preliminary insights into the metabolism of these PCB congeners in pregnant mice. We used liver tissue slices for these studies because the tissue architecture and intercellular communication is maintained in liver tissue slices, which facilitates an extrapolation of our results to the *in vivo* situation.[35, 36] The results show considerable species differences in the PCB metabolite profiles as well as the extent and direction of the atropisomeric enrichment between mice and rats.

EXPERIMENTAL PROCEDURE

Chemicals

Calcium chloride, dimethyl sulfoxide, hexanes, magnesium chloride, methyl *tert*-butyl ether (MTBE), potassium chloride, 2-propanol, sodium chloride, and tetrabutylammonium sulfite were obtained from Fisher Scientific (Pittsburg, PA, USA). Phenobarbital, dexamethasone, sodium dihydrogen phosphate and sodium bicarbonate were purchased from Sigma-Aldrich Co. (St. Louis, MO, USA). HEPES (4-(2-hydroxyethyl)-1-piperazineethanesulfonic acid) and glucose were obtained from Research Products International Corp. (Drive Mount Prospect, IL, USA). 2,2',3,4',6-Pentachlorobiphenyl (PCB 91) ; 2,2',3,5',6-pentachlorobiphenyl (PCB 95); 2,3,4',5,6-pentachlorobiphenyl (PCB 117); 2,2',3,3',4,6'-hexachlorobiphenyl (PCB 132); 2,2',3,4',5',6-hexachlorobiphenyl (PCB 149), 2,3,4,4',5,6-hexachlorobiphenyl (PCB 166), 2,2',3,4,4',5,6,6'-octachlorobiphenyl (PCB 204), 4-OH-2,3,3,4,5,5-hexachlorobiphenyl (4–159) were purchased from AccuStandard (New Haven, CT, USA). 2,2',3,3',6,6'-Hexachlorobiphenyl (PCB 136) and all of the corresponding OH-PCB metabolites were synthesized as described earlier.[22, 24, 37] The chemical structures and abbreviations of the OH-PCBs are shown in Figure 1. Diazomethane was synthesized from *N*-methyl-*N*-nitroso-*p*-toluenesulfonamide (Diazald) using an Aldrich mini Diazald apparatus (Milwaukee, WI, USA). *CAUTION: Because of the highly toxic and explosive nature of diazomethane, its preparation and use should be carried out in an efficient chemical fume hood and behind a safety shield. All glass tubing used to handle diazomethane solutions should have fire polished ends*.

Animals and liver tissue slice preparation

Experiments involving animals were approved by the Institutional Animal Care and Use Committee at the University of Iowa. Female C57BL/6 mice were obtained from Harlan (7-weeks old, Table S1). The mice were housed in a temperature- and light-controlled room with standard diet and tap water *ad libitum*. After a 1–2 week acclimation, the animals were pretreated by intraperitoneal injection with phenobarbital (PB, 102 mg/kg b.w./d in saline

for 3 consecutive days), dexamethasone (DEX, 50 mg/kg b.w./d in corn oil for 4 consecutive days), 0.9% saline (20 mL/kg b.w./d for 3 consecutive days) or corn oil (CO) (10 mL/kg b.w./d for 4 consecutive days) to maximally induce relevant P450 enzymes (i.e., P450 2B for PB-pretreatment and P450 3A and, to a lesser extent, P450 2B for DEX-pretreatment).[27, 38, 39] Twenty-four hours after the last treatment, the animals were euthanized by CO_2 asphyxiation followed by cervical dislocation. Livers were immediately excised and placed in cold Krebs-Henseleit (K-H, pH 7.4) buffer containing 120 mM sodium chloride, 5 mM potassium chloride, 0.5 mM magnesium chloride, 0.8 mM sodium dihydrogen phosphate, 11 mM glucose, 25 mM sodium bicarbonate and 3 mM calcium chloride and 25 mM HEPEs.[28, 40] The liver slices (8 mm in diameter; 200–300 μm thick) were prepared using a Krumdieck tissue slicer (Alabama Research and Development Corporation, Munsford, AL, USA) and collected in ice-cold K-H buffer as described previously.[28, 40]

Two slices per incubation were placed in glass scintillation vials with K-H buffer (2 mL). Ten μL of PCB 91, 95, 132, 136 or 149 solutions in DMSO or DMSO alone (blank sample incubation) were added to each vial, with a final PCB concentration of 50 μM (final DMSO concentration 0.5%). If not stated otherwise, open vials containing the tissue slices were incubated for 4 h at 37°C under an atmosphere of 5% CO_2/95% air in a dynamic incubation system described elsewhere.[40] After incubation, liver slices were washed with cold K-H buffer (1 mL) and homogenized in K-H buffer (3 mL). Aliquots (150 μL) of tissue homogenates and medium were stored at −75 °C for lactate dehydrogenase (LDH) and protein determinations. Sodium hydroxide (0.5 M, 2 or 3 mL) was added to the remaining medium and tissue homogenate samples and the samples were stored at −20 °C prior to PCB and PCB metabolite extraction. Duplication incubations with mouse liver tissue slices were repeated 3 to 5 times. The data are presented as mean ± standard error of mean (SEM) if not stated otherwise.

Assessment of slice viability

The metabolic viability of the liver slices in the culture system, a measure of the tissue quality,[35] was evaluated by measuring the percentage of LDH released into medium using the Cytotoxicity Detection KitPLUS (Roche Applied Sciences, Indianapolis, IN, USA) following manufacturer instructions. LDH release was expressed as percentage of total LDH using the formula % LDH release = $A_1 * D_1 / (A_1 * D_1 + A_2 * D_2)$ (A_1 and A_2: absorbance for medium and homogenate samples, respectively; D_1 and D_2: dilution factor for medium and homogenate samples, respectively).[41]

Extraction of chiral PCBs and their metabolites

All samples were spiked with appropriate recovery standards (500 ng PCB 166 for PCB 136 or 500 ng PCB 117 for all other PCBs; 274 ng 4–159) and extracted as described previously.[28] Blank buffer samples were analyzed in parallel. Briefly, after acidification with 6 M of hydrogen chloride (1 mL) and addition of 2-propanol (3 mL), the medium and homogenate samples were extracted with hexane-MTBE (1:1, v/v, 5 mL) followed by hexanes (3 mL). The combined organic phases were washed by 1% KCl (3 mL), and the KCl phase was washed by hexanes (3 mL). The combined organic phase was dried under a gentle stream of nitrogen. The samples were reconstituted in 1 mL hexanes. After derivatization of the OH-PCBs with diazomethane, the organic extracts were spiked with the appropriate internal standards (250 ng PCB 166 for PCB 149 or 200 ng PCB 204 for PCBs 91, 95,132 and 136). Finally, the organic extracts were subjected to a sulfur clean-up step as described earlier,[39] followed by treatment with concentrated sulfuric acid.

Analysis of chiral PCBs and their metabolites

Levels of PCBs and derivatized OH-PCBs in liver tissue slices were determined with an Agilent 6980N gas chromatograph equipped with a ^{63}Ni μ-electron capture detector (GC-ECD) and a DB-1MS capillary column (60 m × 0.25 mm inner diameter (ID), 0.25 μm film thickness; Supelco, St Louis, MO, USA). This GC method allows a rapid and sensitive quantification of all analytes of interest, including minor OH-PCB metabolites. The injector and detector temperatures were 280 °C and 300 °C, respectively. The temperature program was as follows: 5°C/min from 100 °C to 250 °C, hold for 20 min, 5°C/min to 280 °C, hold for 3 min. The run time was 60 min. Quality assurance/quality control samples analyzed in parallel with each sample set included solvent blanks (instrument contamination control), blank buffer samples and blank sample incubations. PCB and OH-PCB levels were determined using relative response factors obtained from a calibration standard containing all analytes and standards. Subsequently, PCB and OH-PCB levels were adjusted for the percent of the recovery standard recovered from each sample (PCB 166 for PCB 136 and PCB 117 for all other PCB congeners; 4–159 for all OH-PCBs). The recovery rates were 60 ± 9 %, 72 ± 13 % and 78 ± 18 % for PCB 166, PCB 117 and 4–159, respectively. The detector response of all analytes was linear between 1 to 1000 ng/mL ($R^2 > 0.999$). The limits of detection and the levels of PCBs and OH-PCBs in blank medium and tissue slice samples are summarized in the supporting information (Table S2). The amounts of PCBs and hydroxylated metabolites in liver slices were adjusted by protein and incubation time. Protein levels were determined with the method of Lowry[42] using bovine serum albumin as standard.

Metabolite confirmation by mass spectrometry

In order to identify the metabolites formed, the samples were analyzed by electronic ionization on an Agilent 7890A gas chromatograph with a 5975 C mass selective detector (GC-MS) in both total and selective ion monitoring modes with a HP-5 MS column (30 m × 0.32 mm I.D., 0.25 μm film thickness; Agilent, Santa Clara, CA, USA). The temperature program was as follows: 5°C/min from 100 °C to 250 °C, hold for 5 min, 5°C/min to 280 °C, hold for 3 min for hexachlorobiphenyls or 5 °C/min from 100 °C to 280 °C, hold 3 min for pentachlorobiphenyls. The injector, source, quadrupole and transfer line temperatures were 280°C, 230°C, 150°C and 280°C, respectively. In the total scan mode, a mass range of *m/z* 50 to 500 was recorded. The following ions were used in the selected ion monitoring mode: *m/z* 326 for PCBs 91 and 95; *m/z* 360 for PCBs 132, 136 and 149; *m/z* 356 (358) and 386 (388) for mono- and dimethoxylated derivatives of PCB 91 and PCB 95; and *m/z* 390 and 420 for mono- and dimethoxylated derivatives of PCBs 132, 136 and 149.[26]

Atropselective analysis of PCBs and OH-PCBs

Atropisomers of PCBs and major OH-PCB metabolites (as the corresponding methoxylated PCB derivative) were separated on the GC-ECD instrument described above using a ChiralDex BDM column (BDM column, 30 m × 250 μm ID, 0.12 μM film thickness; Supelco, Analytical, St. Louis, MO) for PCB 91, 4–91, 5–91, PCB 95, 5'–132, PCB 149 and 5–149; a Chirasil-Dex column (CD column, 25 m × 0.25 mm ID, 0.25 μM film thickness; Agilent, Santa Clara, CA, USA) for 5– 95, PCB 132, and 5–136; and a Cyclosil-B column (CB column, 30 m × 250 μm ID, 0.25μM film thickness; Agilent, Santa Clara, CA, USA) for PCB 136 and 4–136.[26, 27] Unfortunately, minor OH-PCB metabolites cannot be detected by atropselective GC-ECD analysis. PCBs and their metabolites were separated using the following temperature program: 15 °C/min from 50 to x °C (x = 135 to 160 °C depending on the OH-PCB), hold for up to 544 min at x °C (i.e., until the target analyte eluted from the column), 15 °C/min to 200 °C, and hold for 10 min to clean-out the column. Details of the temperature programs as well as the retention times and resolution of the respective target

analytes are described in the supporting information (Table S3). The flow of carrier gas was 3 mL/min. The chromatograms were integrated using the Valley Drop method.[43] The enantiomeric fraction was calculated with the formula: $EF_{sample} = A_1/(A_1+A_2)$, where A_1 is the peak area of the first eluting atropisomer, and A_2 is the peak area of the second eluting atropisomer. The relative enantiomeric fraction (EF´) values were calculated using the formula: $EF' = EF_{sample}\text{-}EF_{racemic\ standard}$ (the EF values for racemic standards are presented in Table S3).

RESULTS

Optimization of incubation conditions with PCB 136

The effects of PCB concentration (5 to 50 μM), incubation time (2 to 6 h), inducer pretreatment (saline, PB, CO and DEX), and tissue slice viability on the uptake and metabolism of PCB 136 by mouse liver slice were investigated to maximize the formation of OH-PCBs for subsequent atropselective analyses (Figure 2). PCB 136 was selected for these studies because its metabolism and disposition has been extensively studied *in vitro* and *in vivo*.[14, 24, 25, 27–29, 44] The highest PCB 136 concentration investigated (50 μM) was approximately 5-times higher than the apparent K_m reported for PCB 136 metabolism by human liver microsomes (8.8 μM)[25] and, thus, likely to saturate the P450 enzymes in the liver slices. Higher concentrations of PCB 136 were not tested to avoid solubility issues and toxicity (i.e., a reduced viability of the tissue slices). Initial experiments employed liver tissue slices obtained from PB-pretreated female mice. In these experiments, the majority of PCB 136 (85~90%) was detected in the incubation medium. However, the uptake of PCB 136 by the liver tissue slices increased with PCB 136 concentration, with 10 to 15 % total PCB 136 detected in the slices (Figure 2A). The medium to slices ratio of PCB 136, a measure of the uptake of PCB 136 by the tissue slices, ranged from 6.3 to 8.9, with the highest ratio observed at the 50 μM PCB 136 concentration (Figure 2B).

PCB 136 was converted to OH-PCBs in liver slices prepared from PB-pretreated mice, with 5–136 being the major metabolite. Levels of two minor metabolites, 4–136 and 4,5–136, showed some dependence on the PCB concentrations. Levels of 4–136 were higher compared to 4,5–136 at concentrations of 50 μM. (Figure 2C). After 2 h incubation, OH-PCB levels in tissue slices were comparable at PCB 136 concentrations of 5 and 10 μM. However, a 2-fold increase in OH-PCB 136 levels was observed in incubations with 50 μM PCB 136 (Figure 2C). Tissue slices prepared from female mice pretreated with saline, PB, CO or DEX showed similar PCB 136 metabolite profiles, with total OH-PCB as well as individual metabolite levels decreasing in the order PB > DEX > saline ~ CO (Figure 2D). OH-PCB formation rate did not change with incubation time for all three OH-PCB 136 metabolites investigated (Figure 2E).

The viability of liver slices treated with PCB 136 in DMSO decreased with incubation time, with a reduced viability (> 30% LDH release) after 6 h (Figure 2F). Tissue slice viability was not adversely affected by treatment with PCB 136 compared to treatment with DMSO alone in incubations after 4 h (27 ± 8 % versus 26 ± 7 % LDH release, respectively). Based on these results with PCB 136, subsequent metabolism experiments used liver tissue slices from PB pretreated female mice, 4 h incubation times and PCB concentrations of 50 μM to maximize the formation of OH-PCB metabolites, especially 5-OH-PCBs.

PCB levels in liver tissue slices from PB-pretreated female mice

Metabolism studies with mouse liver tissue slices were performed with chiral PCBs 91, 95, 132, 136 and 149 to assess the atropselective formation of OH-PCBs. We were able to account for > 79 % of the total PCB added to the tissue slice incubations (Table S4). Similar

to experiments with PCB 136, a large fraction of PCBs was still present in the medium after 4 h, with medium to tissue slice ratios ranging from 1.7 to 5.1. However, approximately 19 to 46 % of the total PCB was detected in the tissue slices. PCB tissue slice levels ranged from 377 to 822 ng/mg protein, with higher tissue slice levels observed for hexa-compared to penta-chlorinated PCB congeners (Figure 3 and Table S4).

OH-PCB profiles and levels in liver tissue slices and medium

Independent of the PCB congener investigated, < 1% of the total PCB was oxidized to OH-PCBs after 4 h (Table S5). The major metabolite of all PCB congeners investigated had the hydroxyl group in the 5-position of the 2,3,6-trichloro-substituted phenyl ring (Figure 3 and Table S5). The 5-OH-PCB levels in tissue slices, which are an indirect measure of the PCB metabolism rate, decreased in the rank order PCB 149 > PCB 91 > PCB 132 ~ PCB 136 > PCB 95. Approximately 19 to 33% of the 5-OH-PCB metabolites of PCBs 91, 95, 132, 136 and 149 were released into the incubation medium (Table S5). 4-OH-PCB and 4,5-OH-PCB metabolites were minor metabolites accounting for 6.3 to 26.8 % and 5.0 to 5.5 % of the total OH-PCB, respectively (Figure 3 and Table S5). The formation of 5-OH-PCB, 4-OH-PCB and 4,5-OH-PCB metabolites was confirmed by GC-MS in the selective ion monitoring mode for PCBs 132, PCB 136 and PCB 149 (Figure S1–S3). We were unable to confirm the presence of the corresponding metabolites of PCB 91 and PCB 95. The 1,2-shift products of PCBs 91 and 132, which are likely formed via the corresponding PCB epoxide intermediate (Figure 1),[45] were minor metabolites detected by GC-ECD analysis and accounted for < 5.4 % of the sum of OH-PCBs (Table S5). However, only the formation of an 1,2-shift product of PCB 136 could be confirmed by GC-MS after 6 h incubation (Figure S2). All other 1,2-shift products were below the detection limit of the GC-MS method.

In the cases of PCBs 91, 132 and 136, metabolite levels detected in liver slices decreased in the approximate order 5-OH-PCB > 4-OH-PCB > 4,5-OH-PCB. 4',5'–132 could not be quantified because the peak co-elutes with the recovery standard, 4–159, in the GC-ECD analysis. The metabolite profile of PCB 95 also followed the rank order 5–95 > 4–95, with 4,5–95 being below the detection limit. The ratio of 5-OH-PCB : 4-OH-PCB ranged from 2 to 12 and followed the order PCB 136 < PCB 95 < PCB 132 ~ PCB 91 (Table 1). Only 5–149 could be quantified in incubations with PCB 149 due to the unavailability of other PCB 149 metabolites standards; however, two peaks were observed in the GC-ECD and GC-MS analyses that likely correspond to 4–149 and 4,5–149 (Figure S3).

Atropisomeric enrichment of PCBs in mouse liver tissue slices

The atropisomeric enrichment of the PCB congeners in liver tissue slices was determined on appropriate atropselective gas chromatography columns (BDM column for PCBs 91, 95 and 149; CD column for PCB 132; CB column for PCB 136 atropisomers). Despite the high PCB concentration, all PCB congeners displayed slight atropisomeric enrichment in tissue slices, with an enrichment of the second eluting atropisomer of PCBs 95, 132, 136 and 149 and the first eluting atropisomer of PCB 91 (Figure 4). For the PCB 132 and 136, the (−)-atropisomer eluted first on the respective chiral column,[46, 47] which corresponds to an enrichment of (+)-PCB 132 and (+)-PCB 136 in mouse liver tissue slice incubations.

Atropselective formation of OH-PCBs in mouse liver tissue slices

Atropselective gas chromatography was used to assess the atropselective formation of OH-PCB atropisomers (Figure 4; see Figures S4–S8 for representative chromatograms). In mouse liver tissue slices, 4–91, 5–91 and 5'–132 showed an enrichment of the second eluting atropisomer on the BDM column. In contrast, the first eluting atropisomer of 5–149 was enriched on the BDM column. The first eluting atropisomers also displayed enrichment for 5–95 and 5–136 on the CD column and for 4–136 on the CB column. The same enrichment

pattern was also observed for 4–91, 5–91, 5'–132 and 5–149 in the medium. All other metabolites in the medium were below the detection limit of the respective atropselective analysis. EF' values > 0 followed the rank order 5–95 > 5–149 > 5–136, whereas EF' values < 0 followed the rank order, 5'–132 < 5–91.

DISCUSSION

The present study investigated the atropselective oxidation of a series of environmentally relevant, RyR-active PCB congeners in tissue slices obtained from female mice. The objective was to contribute to our understanding of the metabolism of these neurodevelopmental toxicants in a toxicologically relevant animal model. Similar to an earlier *in vitro* metabolism study,[27] the extent of the atropisomeric enrichment of the PCB congeners in the present study was relatively small because only a small percentage of the PCB (< 1 %) was converted to OH-PCBs (i.e., any atropisomeric enrichment is masked by the racemic PCB remaining in the incubation); however, the direction of the enrichment of the PCBs in the present study was in good agreement with animal studies. Specifically, (+)-PCB 136 was enriched in incubations with mouse liver tissue slices prepared from PB-pretreated mice, which is consistent with the PCB 136 enrichment pattern observed in the liver of mice after treatment with racemic PCB 136.[31, 39, 48, 49] Similarly, the enrichment of the first eluting atropisomer of PCB 91 and the second eluting atropisomer of PCBs 95, 132, 136 and 149 in our liver tissue slice incubations was consistent with several animal studies.[21, 50, 51] Studies with other POPs also demonstrate that tissue slice studies can predict the enantiomeric enrichment observed in animal experiments. For example, Ulrich et al. demonstrated that liver tissue slices from PB-pretreated rats resulted in an enantiomeric enrichment of (−)-α-hexachlorohexane (EF = 0.43).[52] A similar EF value of 0.44 was observed in the same study in the liver of PB-pretreated rats dosed subcutaneously with racemic α-hexachlorohexane. *In vitro* studies were also predictive of the enrichment of (−)-PCB 136 in rats[22, 27–29] and the *R*-(−)-enantiomer of the fungicide benalaxyl in rainbow trout.[53]

The atropisomeric enrichment of PCBs in adult mice and other mammals, including humans, is due to their atropselective metabolism to OH-PCBs and other metabolites by P450 enzymes.[14] Analogous to the present study, several earlier studies demonstrate that the chiral PCB congeners investigated in this study are typically oxidized in the 4- and 5-position of the 2,3,6-trichloro substituted phenyl ring by mammalian P450 enzymes (Figure 1). In addition, a chiral 1,2-shift product with a 2,4,6-trichloro-3-hydroxy substitution pattern can be formed as a minor metabolite in mammals. The oxidation of chiral PCBs in the 5-position is catalyzed by P450 2B enzymes[24, 29] and occurs by direct insertion of oxygen into an aromatic C-H bond.[54] These earlier observations are in agreement with our observation that 5-OH-PCBs are preferentially formed in tissue slices from PB- and DEX-pretreated mice (with PB > DEX). The formation of the 4-OH-PCB and 1,2-shift metabolites involves currently unidentified mammalian P450 isoforms and is thought to occur via an arene oxide intermediate.[54] Our study suggests that, similar to rats,[27, 28] P450 3A enzymes are not involved in the formation of both OH-PCB metabolites in mice because their levels were not altered in incubations using tissue slices from DEX-pretreated mice. It is interesting to note that the P450 2B–catalyzed oxidation of chiral PCBs, such as PCB 91, in mice apparently occurs in the higher chlorinated phenyl ring with a 2,3,6-trichloro substitution pattern. In contrast, the unchlorinated phenyl rings of di-*ortho* substituted, lower chlorinated PCBs are preferentially oxidized by rat P450 2B enzymes.[55]

Structure-activity relationships studies demonstrate that the position of the hydroxyl group (i.e., *meta* vs. *para*) plays an important role in the interaction of OH-PCB with cellular targets (i.e., RyRs) implicated in PCBs' developmental neurotoxicity.[8, 18, 19] These

mechanistic studies suggest that the levels of 5-OH-PCB and 4-OH-PCB metabolites present *in vivo* may play a role in the developmental neurotoxicity of PCBs. Comparison of the 5-OH-PCB : 4-OH-PCB ratios for the chiral PCB congeners reported by in this and other *in vitro* studies revealed considerable congener and species differences, especially in experiments using tissue slices or microsomes from PB-pretreated animals (Table 1). In incubations using liver tissue slices from PB-pretreated mice, 5-OH-PCBs were the major metabolites, with relatively small 5-OH-PCB : 4-OH-PCB ratios ranging from 2 : 1 to 12 : 1 for the different PCB congeners investigated. These ratios are close to the 1 : 1 ratio observed in metabolism studies using pooled human liver microsomes.[25] In liver microsomes and tissue slices from mice and rats, the 5-OH-PCB : 4-OH-PCB ratio increased with the induction of P450 2B enzymes following DEX and PB-pretreatment (i.e., naïve animals or vehicle < DEX < PB pretreatment).[26–28] However, the increase in the 5–136 : 4–136 ratio was much more pronounced in incubations using microsomes or tissue slices obtained from rat compared to mouse livers. For example, the 5–136 : 4–136 ratio observed in incubation with microsomes prepared from PB-pretreated rats was 137 : 1.[27] This species difference in the relative formation of 5–136 versus 4–136 is consistent with the more pronounced maximal induction of P450 2B enzyme activities compared to constitutive activities in rats versus mice following inducer pretreatment.[56]

5-OH-PCB and 4-OH-PCB levels have also been reported for several animal studies. 5–95 was the major metabolite observed in mice and rats treated orally with PCB 95.[57] 5–136 also was the major metabolite in male and female rats treated intraperitoneally with PCB 136, with 5–136 : 4–136 ratios of 5 : 1 and 6 : 1 for male and female rats, respectively.[22] In mice, the 5-OH-PCB : 4-OH-PCB ratio in the liver and blood was dose-dependent following subchronic oral exposure to PCB 95.[21] Briefly, 5–95 was the major metabolite in the liver of mice treated subchronically with low doses PCB 95, whereas 4–95 was the major metabolite in animals receiving higher doses of PCB 95. 4–95 was also the major metabolite in blood; however, the relative levels of 5–95 increased with increasing PCB 95 dose. These differences in the metabolite profiles between the tissue slice and *in vivo* data demonstrate that complex factors, for example the experimental design (e.g. dose of PCB), induction of P450 enzymes and further metabolism *via* conjugation reactions, govern the disposition of chiral OH-PCBs in toxicologically relevant animal models.

All five PCB congeners investigated in the present study are known to undergo congener- and species-specific atropisomeric enrichment in wildlife;[14] however, there is currently limited evidence that different PCB congeners and their OH-PCB metabolites undergo species-dependent atropisomeric enrichment in different rodent species. Our study reveals several, congener-specific differences in the direction of the atropisomeric enrichment of PCBs and OH-PCBs between mice and rats. Specifically, the direction of the atropisomeric enrichment of PCBs 95 and 136 as well as OH-PCBs 5–95 and 5–136 in experiments using liver microsomes obtained from PB-pretreated rats[26, 27] is opposite to the enrichment observed in our mouse liver tissue slice experiments; however, the direction of the atropisomeric enrichment in both species was identical for PCBs 91, 132 and 149 and OH-PCBs 5–91, 5'–132, 4–136 and 5–149. Furthermore, the extent of the atropisomeric enrichment of the OH-PCB metabolites appears to be greater in mice compared to rats.

Although our study was performed using tissue slices obtained from adult mice, our results provide some insights into a potential role of P450 2B induction on the metabolism of PCB during gestation. As shown by Lucier and co-workers for PCB 136 in rats, OH-PCBs are formed in the maternal but not the fetal compartment.[23] The OH-PCBs cross the placental barrier and accumulate in the fetal intestine as the corresponding glucuronides. Subsequently, the OH-PCB conjugates can be deconjugated and undergo enterohepatic circulation in the fetus. Fetal accumulation of OH-PCB have also been documented for 3,3',

4,4'-tetrachlorobiphenyl (PCB 77) in rats.[58] Since developmental toxicity studies in rodents showed an increase in P450 2B enzyme activity in dams following exposure to PCB mixtures,[59, 60] the increased maternal metabolism of chiral PCBs to potentially neurotoxic OH-PCBs is expected to increase the extent of OH-PCB accumulation in the fetus.

Our study demonstrates that PCBs are atropselectively metabolized to chiral 5-OH-PCB and 4-OH-PCB metabolites in mouse liver tissue slices. Comparison of the metabolites profiles with similar experiments using rat liver microsomes or tissue slices revealed considerable differences in the metabolite ratios and chiral signatures of the parent PCB and its OH-PCB metabolites between mice and rats. Furthermore, hepatic induction of P450 2B enzymes by PB and DEX influenced metabolite profiles in a species-dependent manner, with drastically higher 5-OH-PCB to 4-OH-PCB ratios observed in rats compared to mice. Based on these observations, we hypothesize that the toxicokinetics of PCB and OH-PCB atropisomers differs between mice and rats and can be modulated by the induction of P450 2B enzymes in a species dependent manner. Further studies are therefore warranted to assess the effect of species and P450 2B induction on levels, profiles and chiral signatures of PCBs and OH-PCBs during developmentally sensitive periods, with the ultimate goal of understanding of the role of PCB metabolism in the developmental neurotoxicity of PCBs in different species, especially humans.

Supplementary Material

Refer to Web version on PubMed Central for supplementary material.

Acknowledgments

The authors thank E.A. Mash and S.C. Waller of the Synthetic Chemistry Facility Core of the Southwest Environmental Health Sciences Center for a generous gift of the hydroxylated PCB 136 metabolites.

FUNDING SOURCES

This work was supported by grants ES05605, ES013661 and ES017425 from the National Institute of Environmental Health Sciences, National Institutes of Health. The synthesis of several hydroxylated PCB 136 standards was funded by NIH grant ES06694. The content is solely the responsibility of the authors and does not necessarily represent the official views of the National Institute of Environmental Health Sciences or the National Institutes of Health.

ABBREVIATIONS

AhR	aryl hydrocarbon receptor
BDM	ChiralDex BDM column
CB	Cyclosil-B column
CD	Chirasil-Dex column
CO	corn oil
DEX	dexamethasone
DMSO	dimethyl sulfoxide
EF	enantiomeric fraction
EF´	relative enantiomeric fraction
GC-ECD	gas chromatograph equipped with electron capture detector
GC-MS	gas chromatograph with mass selective detector

HEPES	4-(2-hydroxyethyl)-1-piperazineethanesulfonic acid
ID	inner diameter
K-H	Krebs-Henseleit buffer
LDH	lactate dehydrogenase
MTBE	methyl *tert*-butyl ether
PCBs	polychlorinated biphenyls
PCB 91	2,2',3,4',6-pentachlorobiphenyl
PCB 95	2,2',3,5',6-pentachlorobiphenyl
PCB 132	2,2',3,3',4,6'-hexachlorobiphenyl
PCB 136	2,2',3,3',6,6'-hexachlorobiphenyl
PCB 149	2,2',3,4',5',6-hexachlorobiphenyl
OH-PCB	hydroxylated polychlorinated biphenyl metabolite
PB	phenobarbital
POPs	persistent organic pollutants
RyR	Ryanodine receptor
SEM	standard error of mean

REFERENCES

1. Grandjean P, Landrigan PJ. Developmental neurotoxicity of industrial chemicals. Lancet. 2006; 368:2167–2178. [PubMed: 17174709]
2. Scientific Frontiers in Developmental Toxicology and Risk Assessment. Washington, DC: National Research Council, The National Academies Press; 2000.
3. Carpenter DO. Polychlorinated biphenyls (PCBs): routes of exposure and effects on human health. Rev. Environ. Health. 2006; 21:1–23. [PubMed: 16700427]
4. Korrick SA, Sagiv SK. Polychlorinated biphenyls, organochlorine pesticides and neurodevelopment. Curr. Opin. Pediatr. 2008; 20:198–204. [PubMed: 18332718]
5. Bandiera S, Safe S, Okey AB. Binding of polychlorinated biphenyls classified as either phenobarbitone, 3-methylcholanthrene or mixed-type inducers to cytosolic Ah receptor. Chem.-Biol. Interact. 1982; 39:259–277. [PubMed: 6804100]
6. Mariussen E, Fonnum F. Neurochemical targets and behavioral effects of organohalogen compounds: An update. Crit. Rev. Toxicol. 2006; 36:253–289. [PubMed: 16686424]
7. Pessah IN, Cherednichenko G, Lein PJ. Minding the calcium store: Ryanodine receptor activation as a convergent mechanism of PCB toxicity. Pharmacol. Ther. 2010; 125:260–285. [PubMed: 19931307]
8. Pessah IN, Hansen LG, Albertson TE, Garner CE, Ta TA, Do Z, Kim KH, Wong PW. Structure-activity relationship for noncoplanar polychlorinated biphenyl congeners toward the ryanodine receptor-Ca^{2+} channel complex type 1 (RyR1). Chem. Res. Toxicol. 2006; 19:92–101. [PubMed: 16411661]
9. Wayman GA, Yang D, Bose DD, Lesiak A, Ledoux V, Bruun D, Pessah IN, Lein PJ. PCB-95 promotes dendritic growth via ryanodine receptor-dependent mechanisms. Environ. Health Perspect. 2012; 120:997–1002. [PubMed: 22534141]
10. Yang D, Kim KH, Phimister A, Bachstetter AD, Ward TR, Stackman RW, Mervis RF, Wisniewski AB, Klein SL, Kodavanti PR, Anderson KA, Wayman G, Pessah IN, Lein PJ. Developmental exposure to polychlorinated biphenyls interferes with experience-dependent dendritic plasticity

and ryanodine receptor expression in weanling rats. Environ. Health Perspect. 2009; 117:426–435. [PubMed: 19337518]

11. Kostyniak PJ, Hansen LG, Widholm JJ, Fitzpatrick RD, Olson JR, Helferich JL, Kim KH, Sable HJK, Seegal RF, Pessah IN, Schantz SL. Formulation and characterization of an experimental PCB mixture designed to mimic human exposure from contaminated fish. Toxicol. Sci. 2005; 88:400–411. [PubMed: 16177234]
12. Frame GM, Cochran JW, Bowadt SS. Complete PCB congener distributions for 17 Aroclor mixtures determined by 3 HRGC systems optimized for comprehensive, quantitative, congener-specific analysis. J. High. Resolut. Chromatogr. 1996; 19:657–668.
13. Frame GM, Wagner RE, Carnahan JC, Brown JF Jr, May RJ, Smullen LA, Bedard DL. Comprehensive, quantitative congener-specific analyses of eight Aroclors and complete PCB congener assignments on DB-1 capillary GC columns. Chemosphere. 1996; 33:603–623.
14. Lehmler H-J, Harrad SJ, Huhnerfuss H, Kania-Korwel I, Lee CM, Lu Z, Wong CS. Chiral polychlorinated biphenyl transport, metabolism, and distribution: A review. Environ. Sci. Technol. 2010; 44:2757–2766. [PubMed: 20384371]
15. Pessah IN, Lehmler H-J, Robertson LW, Perez CF, Cabrales E, Bose DD, Feng W. Enantiomeric specificity of (−)-2,2',3,3',6,6'-hexachlorobiphenyl toward ryanodine receptor types 1 and 2. Chem. Res. Toxicol. 2009; 22:201–207. [PubMed: 18954145]
16. Lehmler H-J, Robertson LW, Garrison AW, Kodavanti PRS. Effects of PCB 84 enantiomers on [^{3}H] phorbol ester binding in rat cerebellar granule cells and $^{45}Ca^{2+}$-uptake in rat cerebellum. Toxicol. Lett. 2005; 156:391–400. [PubMed: 15763638]
17. Park HY, Park JS, Sovcikova E, Kocan A, Linderholm L, Bergman A, Trnovec T, Hertz-Picciotto I. Exposure to hydroxylated polychlorinated biphenyls (OH-PCBs) in the prenatal period and subsequent neurodevelopment in eastern Slovakia. Environ Health Perspect. 2009; 117:1600–1606. [PubMed: 20019912]
18. Kodavanti PRS, Ward TR, Derr-Yellin EC, McKinney JD, Tilson HA. Increased [^{3}H]phorbol ester binding in rat cerebellar granule cells and inhibition of $^{45}Ca^{2+}$ buffering in rat cerebellum by hydroxylated polychlorinated biphenyls. Neurotoxicology. 2003; 24:187–198. [PubMed: 12606291]
19. Niknam Y, Feng W, Cherednichenko G, Dong Y, Joshi SN, Vyas SM, Lehmler H-J, Pessah IN. Structure-activity relationship of select meta- and para-hydroxylated non-dioxin-like polychlorinated biphenyls: from single RyR1 channels to muscle dysfunction. Toxicol. Sci. 2013
20. Meerts IA, Assink Y, Cenijn PH, Van Den Berg JH, Weijers BM, Bergman A, Koeman JH, Brouwer A. Placental transfer of a hydroxylated polychlorinated biphenyl and effects on fetal and maternal thyroid hormone homeostasis in the rat. Toxicol. Sci. 2002; 68:361–371. [PubMed: 12151632]
21. Kania-Korwel I, Barnhart CD, Stamou M, Truong KM, El-Komy MH, Lein PJ, Veng-Pedersen P, Lehmler H-J. 2,2',3,5',6-Pentachlorobiphenyl (PCB 95) and its hydroxylated metabolites are enantiomerically enriched in female mice. Environ. Sci. Technol. 2012; 46:11393–11401. [PubMed: 22974126]
22. Kania-Korwel I, Vyas SM, Song Y, Lehmler H-J. Gas chromatographic separation of methoxylated polychlorinated biphenyl atropisomers. J. Chromatogr. A. 2008; 1207:146–154. [PubMed: 18760792]
23. Lucier GW, McDaniel OS, Schiller CM, Matthews HB. Structural requirements for the accumulation of chlorinated biphenyl metabolites in the fetal rat intestine. Drug Metab. Dispos. 1978; 6:584–590. [PubMed: 30609]
24. Waller SC, He YA, Harlow GR, He YQ, Mash EA, Halpert JR. 2,2',3,3',6,6'-Hexachlorobiphenyl hydroxylation by active site mutants of cytochrome P450 2B1 and 2B11. Chem. Res. Toxicol. 1999; 12:690–699. [PubMed: 10458702]
25. Schnellmann RG, Putnam CW, Sipes IG. Metabolism of 2,2',3,3',6,6'-hexachlorobiphenyl and 2,2',4,4',5,5'-hexachlorobiphenyl by human hepatic microsomes. Biochem Pharmacol. 1983; 32:3233–3239. [PubMed: 6416258]

26. Kania-Korwel I, Duffel MW, Lehmler H-J. Gas chromatographic analysis with chiral cyclodextrin phases reveals the enantioselective formation of hydroxylated polychlorinated biphenyls by rat liver microsomes. Environ. Sci. Technol. 2011; 45:9590–9596. [PubMed: 21966948]
27. Wu X, Pramanik A, Duffel MW, Hrycay EG, Bandiera SM, Lehmler H-J, Kania-Korwel I. 2,2', 3,3',6,6'-Hexachlorobiphenyl (PCB 136) is enantioselectively oxidized to hydroxylated metabolites by rat liver microsomes. Chem. Res. Toxicol. 2011; 24:2249–2257. [PubMed: 22026639]
28. Wu X, Kania-Korwel I, Chen H, Stamou M, Dammanahalli KJ, Duffel M, Lein PJ, Lehmler H-J. Metabolism of 2,2',3,3',6,6'-hexachlorobiphenyl (PCB 136) atropisomers in tissue slices from phenobarbital or dexamethasone-induced rats is sex-dependent. Xenobiotica. 2013; 43:933–947. [PubMed: 23581876]
29. Warner NA, Martin JW, Wong CS. Chiral polychlorinated biphenyls are biotransformed enantioselectively by mammalian cytochrome P-450 isozymes to form hydroxylated metabolites. Environ. Sci. Technol. 2009; 43:114–121. [PubMed: 19209593]
30. Lu Z, Wong CS. Factors affecting phase I stereoselective biotransformation of chiral polychlorinated biphenyls by rat cytochrome P-450 2B1 isozyme. Environ. Sci. Technol. 2011; 45:8298–8305. [PubMed: 21863805]
31. Kania-Korwel I, Shaikh NS, Hornbuckle KC, Robertson LW, Lehmler H-J. Enantioselective disposition of PCB 136 (2,2',3,3',6,6'-hexachlorobiphenyl) in C57BL/6 mice after oral and intraperitoneal administration. Chirality. 2007; 19:56–66. [PubMed: 17089340]
32. Schwartzer JJ, Koenig CM, Berman RF. Using mouse models of autism spectrum disorders to study the neurotoxicology of gene-environment interactions. Neurotoxicol Teratol. 2013; 36:17–35. [PubMed: 23010509]
33. Robertson HR, Feng G. Annual Research Review: Transgenic mouse models of childhood-onset psychiatric disorders. J. Child Psychol Psychiatry. 2011; 52:442–475. [PubMed: 21309772]
34. Curran CP, Nebert DW, Genter MB, Patel KV, Schaefer TL, Skelton MR, Williams MT, Vorhees CV. In utero and lactational exposure to PCBs in mice: adult offspring show altered learning and memory depending on Cyp1a2 and Ahr genotypes. Environ Health Perspect. 2011; 119:1286–1293. [PubMed: 21571617]
35. Fisher RL, Vickers AE. Preparation and culture of precision-cut organ slices from human and animal. Xenobiotica. 2013; 43:8–14. [PubMed: 23030812]
36. Lake BG, Price RJ. Evaluation of the metabolism and hepatotoxicity of xenobiotics utilizing precision-cut slices. Xenobiotica. 2013; 43:41–53. [PubMed: 23131042]
37. Joshi SN, Vyas SM, Duffel MW, Parkin S, Lehmler H-J. Synthesis of sterically hindered polychlorinated biphenyl derivatives. Synthesis. 2011:1045–1054. [PubMed: 21516177]
38. Robertson LW, Parkinson A, Bandiera S, Lambert I, Merrill J, Safe SH. PCBs and PBBs: Biologic and toxic effects on C57BL/6J and DBA/2J inbred mice. Toxicology. 1984; 31:191–206. [PubMed: 6330936]
39. Kania-Korwel I, Xie W, Hornbuckle KC, Robertson LW, Lehmler H-J. Enantiomeric enrichment of 2,2',3,3',6,6'-hexachlorobiphenyl (PCB 136) in mice after induction of CYP enzymes. Arch. Environ. Contam. Toxicol. 2008; 55:510–517. [PubMed: 18437444]
40. Dammanahalli JK, Duffel MW. Oxidative modification of rat sulfotransferase 1A1 activity in hepatic tissue slices correlates with effects on the purified enzyme. Drug Metab. Dispos. 2012; 40:298–303. [PubMed: 22041107]
41. Valentovic MA, Ball JG, Anestis DK, Rankin GO. Comparison of the in vitro toxicity of dichloroaniline structural isomers. Toxicol. In Vitro. 1995; 9:75–81. [PubMed: 20650065]
42. Lowry OH, Rosebrough NJ, Farr L, Randall RJ. Protein measurement with the Folin phenol reagent. J. Biol. Chem. 1951; 193:265–275. [PubMed: 14907713]
43. Asher BJ, D'Agostino LA, Way JD, Wong CS, Harynuk JJ. Comparison of peak integration methods for the determination of enantiomeric fraction in environmental samples. Chemosphere. 2009; 75:1042–1048. [PubMed: 19215960]
44. Birnbaum LS. Distribution and excretion of 2,3,6,2',3',6'- and 2,4,5,2',4',5'-hexachlorobiphenyl in senescent rats. Toxicol. Appl. Pharmacol. 1983; 70:262–272. [PubMed: 6414105]
45. Guroff G, Daly JW, Jerina DM, Renson J, Witkop B, Udenfriend S. Hydroxylation-induced migration. NIH shift. Science. 1967; 157:1527–1530.

46. Haglund P, Wiberg K. Determination of the gas chromatographic elution sequences of the (+)- and (−)-enantiomers of stable atropisomeric PCBs on Chirasil-Dex. J. High Res. Chromatogr. 1996; 19:373–376.
47. Kania-Korwel I, Lehmler H-J. Assigning atropisomer elution orders using atropisomerically enriched polychlorinated biphenyl fractions generated by microsomal metabolism. J. Chromatogr. A. 2013; 1278:133–144. [PubMed: 23347976]
48. Kania-Korwel I, Hornbuckle KC, Robertson LW, Lehmler H-J. Dose-dependent enantiomeric enrichment of 2,2',3,3',6,6'-hexachlorobiphenyl in female mice. Environ. Toxicol. Chem. 2008; 27:299–305. [PubMed: 18348647]
49. Kania-Korwel I, Hornbuckle KC, Robertson LW, Lehmler H-J. Influence of dietary fat on the enantioselective disposition of 2,2',3,3',6,6'-hexachlorobiphenyl (PCB 136) in female mice. Food Chem. Toxicol. 2008; 46:637–644. [PubMed: 17950514]
50. Kania-Korwel I, El-Komy MHME, Veng-Pedersen P, Lehmler H-J. Clearance of polychlorinated biphenyl atropisomers is enantioselective in female C57Bl/6 mice. Environ. Sci. Technol. 2010; 44:2828–2835. [PubMed: 20384376]
51. Milanowski B, Lulek J, Lehmler H-J, Kania-Korwel I. Assessment of the disposition of chiral polychlorinated biphenyls in female mdr 1a/b knockout versus wild-type mice using multivariate analyses. Environ. Int. 2010; 36:884–892. [PubMed: 19923000]
52. Ulrich EM, Willett KL, Caperell-Grant A, Bigsby RM, Hites RA. Understanding enantioselective processes: a laboratory rat model for alpha-hexachlorocyclohexane accumulation. Environ. Sci. Technol. 2001; 35:1604–1609. [PubMed: 11329709]
53. Gu X, Yao T. The integration of in vivo and in vitro metabolism assays to investigate the stereoselective behaviors of benalaxyl in rainbow trout (Oncorhynchus mykiss). J. Environ. Sci. Health B. 2013; 48:693–699. [PubMed: 23638897]
54. Preston BD, Miller JA, Miller EC. Non-arene oxide aromatic ring hydroxylation of 2,2',5,5'-tetrachlorobiphenyl as the major metabolic pathway catalyzed by phenobarbital-induced rat liver microsomes. J. Biol. Chem. 1983; 258:8304–8311. [PubMed: 6408087]
55. Kaminsky LS, Kennedy MW, Adams SM, Guengerich FP. Metabolism of dichlorobiphenyls by highly purified isozymes of rat liver cytochrome P-450. Biochemistry. 1981; 20:7379–7384. [PubMed: 6798990]
56. Weaver RJ, Thompson S, Smith G, Dickins M, Elcombe CR, Mayer RT, Burke MD. A comparative study of constitutive and induced alkoxyresorufin O-dealkylation and individual cytochrome P450 forms in cynomolgus monkey (Macaca fascicularis), human, mouse, rat and hamster liver microsomes. Biochem Pharmacol. 1994; 47:763–773. [PubMed: 8135852]
57. Sundström G, Jansson B. The metabolism of 2,2',3,5',6-pentachlorobiphenyl in rats, mice and quails. Chemosphere. 1975; 4:361–370.
58. Morse DC, Wehler EK, van de Pas M, de Bie AT, van Bladeren PJ, Brouwer A. Metabolism and biochemical effects of 3,3',4,4'-tetrachlorobiphenyl in pregnant and fetal rats. Chem. Biol. Interact. 1995; 95:41–56. [PubMed: 7697753]
59. Bonfanti P, Comelli F, Assi L, Casati L, Colciago A, Villa S, Santagostino A, Costa B, Colombo A. Responsiveness of hepatic and cerebral cytochrome P450 in rat offspring prenatally and lactationally exposed to a reconstituted PCB mixture. Environ. Toxicol. 2012:1–11. [PubMed: 20725936]
60. Welsch F. Effects of acute or chronic polychlorinated biphenyl ingestion on maternal metabolic homeostasis and on the manifestations of embryotoxicity caused by cyclophosphamide in mice. Arch. Toxicol. 1985; 57:104–113. [PubMed: 3927875]

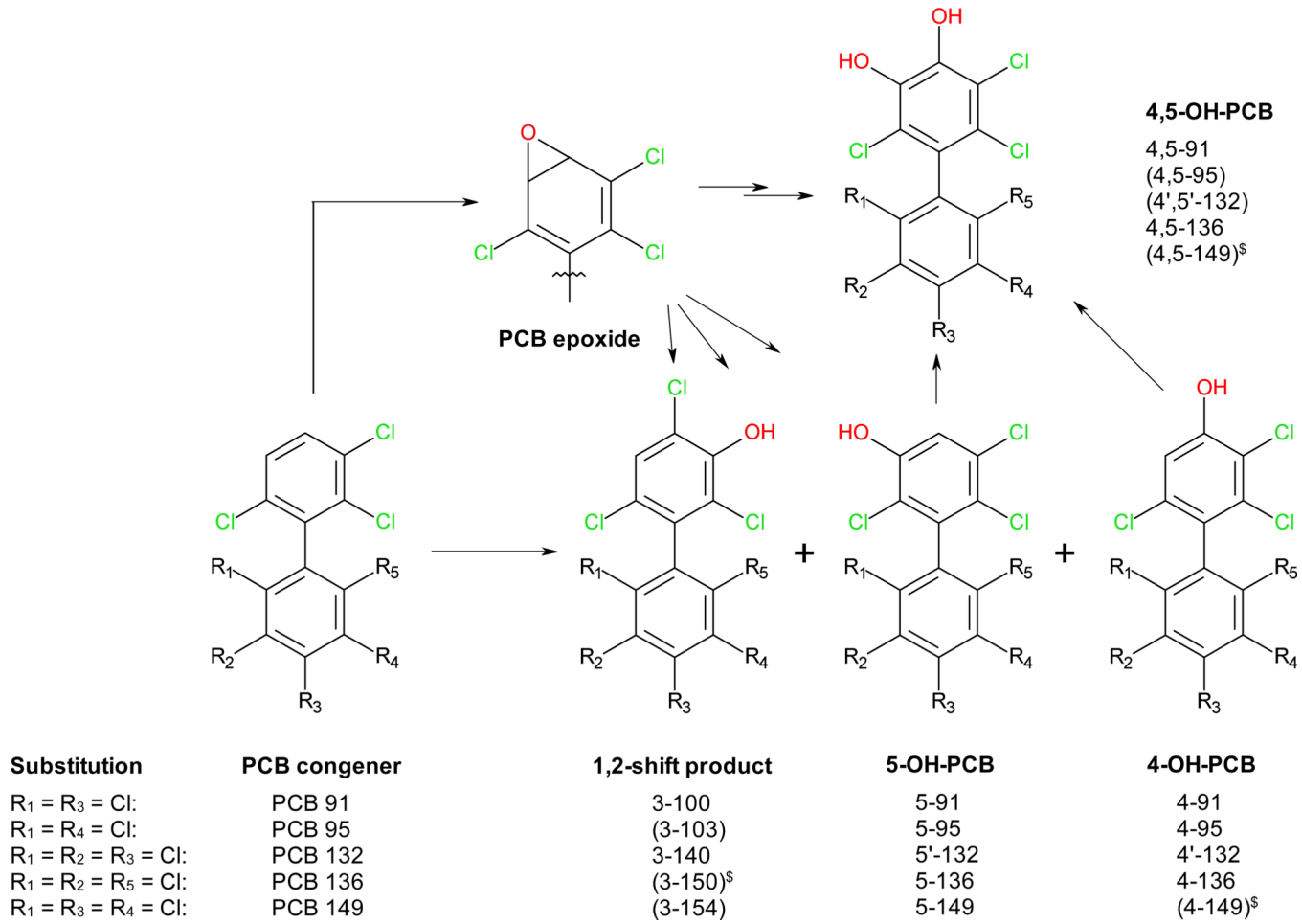

Substitution	PCB congener	1,2-shift product	5-OH-PCB	4-OH-PCB
$R_1 = R_3 = Cl$:	PCB 91	3-100	5-91	4-91
$R_1 = R_4 = Cl$:	PCB 95	(3-103)	5-95	4-95
$R_1 = R_2 = R_3 = Cl$:	PCB 132	3-140	5'-132	4'-132
$R_1 = R_2 = R_5 = Cl$:	PCB 136	(3-150)$	5-136	4-136
$R_1 = R_3 = R_4 = Cl$:	PCB 149	(3-154)	5-149	(4-149)$

Figure 1.

Simplified metabolism scheme showing putative hydroxylated metabolites (OH-PCBs) of chiral PCBs formed by mouse liver tissue slices and the OH-PCB abbreviations used in this study. Metabolites in parentheses were not detected or below the detection limit in the GC-ECD analysis (see Table S5). $ OH-PCBs were tentatively identified by GC-MS analysis.

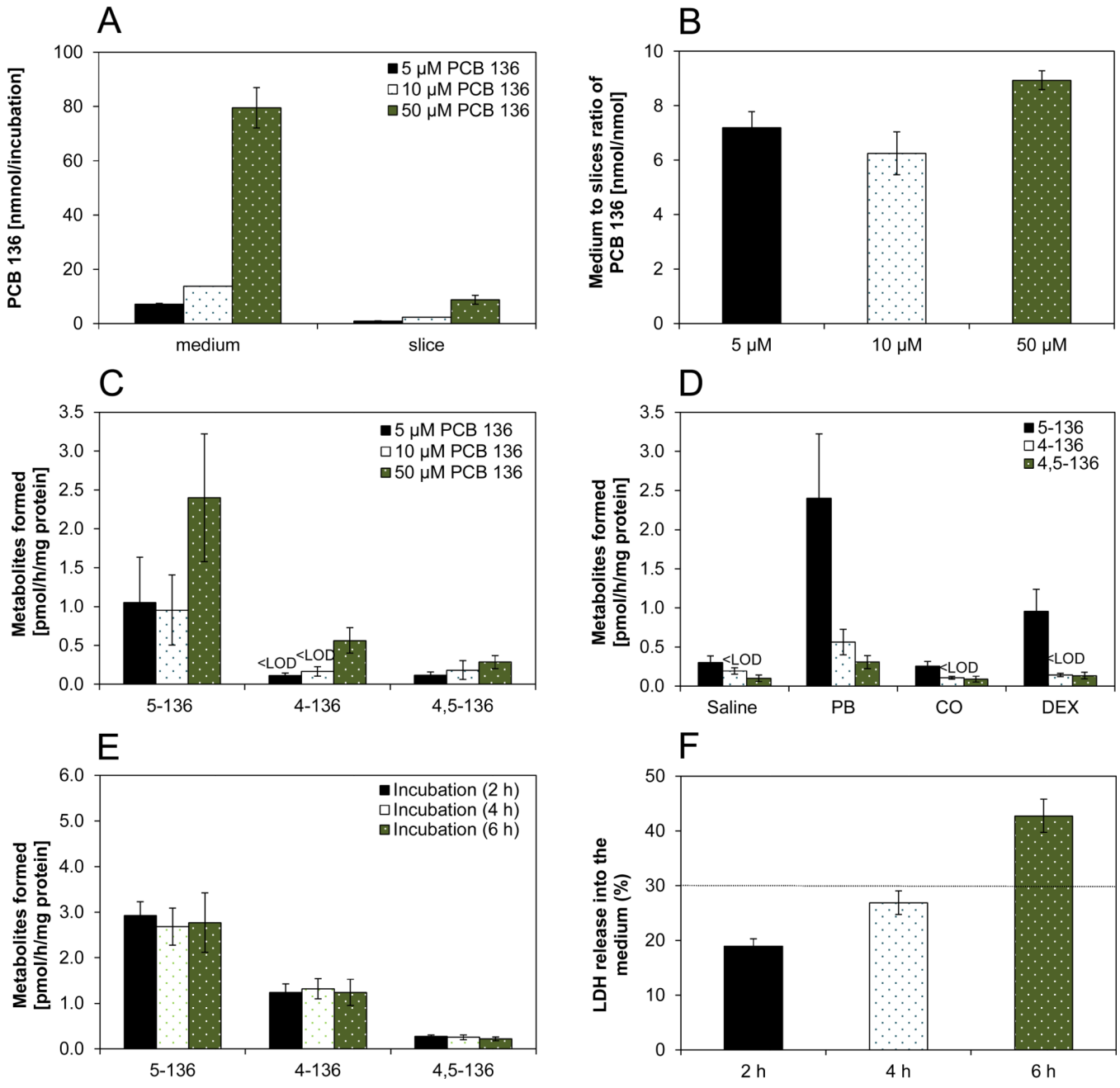

Figure 2.

Optimization of PCB metabolism experiments using liver tissue slices prepared from female mice suggests that incubations for 4 hour with 50 µM PCB provides the highest OH-PCB metabolite levels while maintaining tissue slice viability. A) Uptake of PCB 136 by liver tissue slices prepared from phenobarbital (PB)-pretreated mice over a 2 h incubation period; B) medium to slices ratio of PCB 136 in 2 h incubations with tissue slices prepared from PB-pretreated mice; C) concentration-dependent oxidation of PCB 136 in 2 h incubations with tissue slices prepared from PB-pretreated mice; D) oxidation of PCB 136 in 2 h incubations using tissue slices from saline-, PB-, corn oil (CO) and dexamethasone (DEX)-pretreated mice (50 µM PCB 136); E) rate of formation of OH-PCB 136 metabolites in slices obtained from PB-pretreated mice (50 µM PCB 136) at 2 to 6 h; F) time-dependent

release of LDH from tissue slices obtained from PB-pretreated mice into medium after PCB treatment (50 μM PCB 136). As indicated by the dotted line, tissue slices were considered viable if the LDH release was below 30%. All values were mean ± standard error of mean (3 to 5 mouse livers for each treatment).

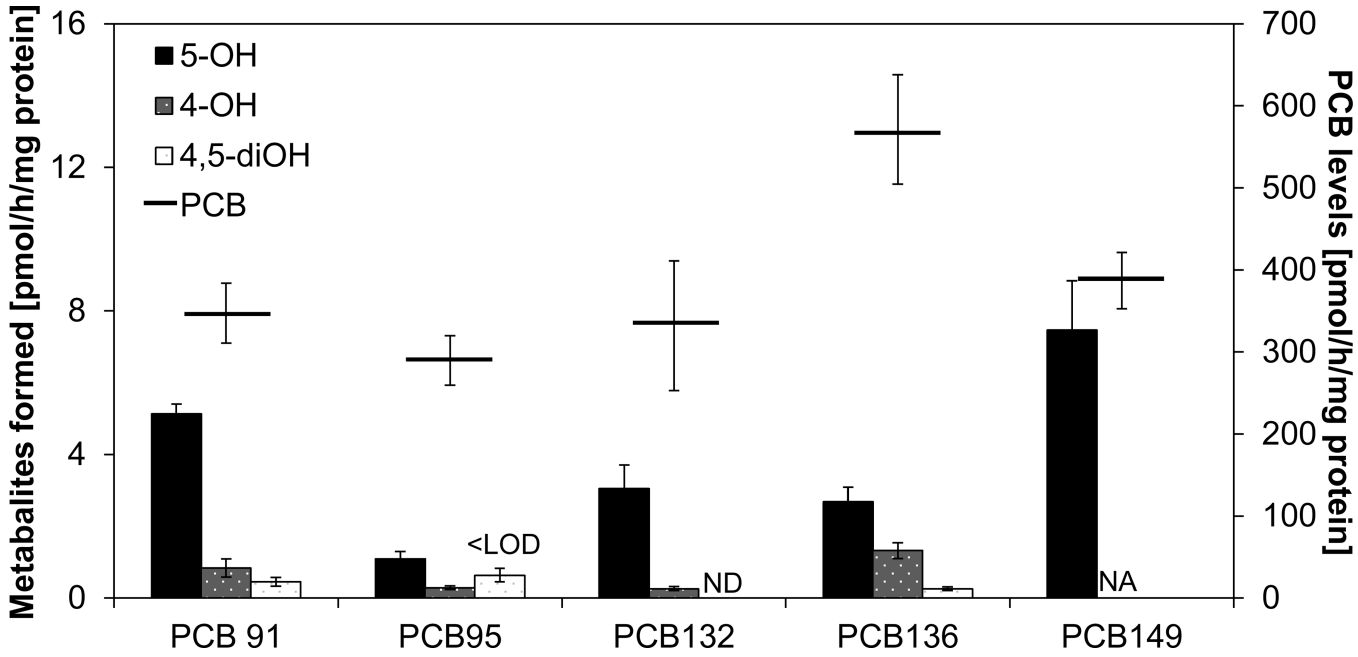

Figure 3.

The levels of PCBs 91, 95, 132, 136 and 149 and their hydroxylated metabolites detected in liver slices prepared from PB-pretreated mice. The major metabolite of all PCB congeners investigated had the hydroxyl group in 5-position of the 2,3,6-trichloro-substituted phenyl ring. Incubations of the parent PCBs with liver tissue slices from PB-pretreated mice were performed at least in triplicate for 4 h at 50 μM PCB. PCBs and OH-PCBs were extracted and qualified by gas chromatography as described under Experimental Procedure. LOD: Limit of detection; NA: not applicable (no standards); ND: Not detected. The values are means ± standard error of mean.

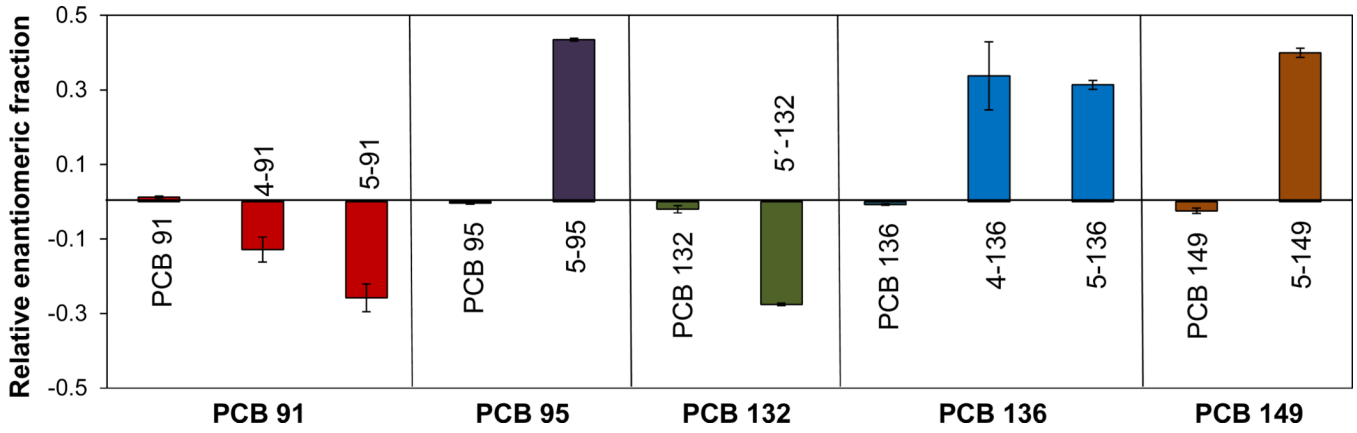

Figure 4.

The relative enantiomeric fractions (EF') of PCBs 91, 95, 132, 136 and 149 and their hydroxylated metabolites from mouse liver slice incubations. The EF' values were calculated using the formula EF' = EF_{sample}-$EF_{racemic\ standard}$ as sescribed under Experimental Procedure. Atropisomers were separated on a BDM column for PCB 91, 4–91, 5–91, PCB 95, 5'–132, PCB 149 and 5–149; on a Chirasil-Dex column for 5–95, PCB 132, and 5–136; on a Cyclosil-B column for PCB 136 and 4–136 as described under Experimental Procedure. The values are mean ± standard deviation.

Table 1

Comparison of 5-OH-PCB : 4-OH-PCB ratios observed in metabolism studies using of liver microsomes or tissue slices obtained from mice, rats or humans.

Species	Microsomes or tissue slices	Sex	PCB 91	PCB 95	PCB 132	PCB 136		
						Pretreatment		
						Vehicle or Naïve	Dexamethasone	Phenobarbital
Mice	Liver slices	Female	12	4	11	-	-	2
Rats	Liver slices*	Female	-	-	-	0.4	11	17
		Male	-	-	-	0.7	19	59
	Microsomes#	Male	100	nd	17	5	43	137
Human	Microsomes&	Pooled	-	-	-	1	-	-

*Data from Wu et al.:[28]

Rat liver tissue slices from PB-pretreated animals were incubated with PCB 136 for 2 h.

#Data from Wu et al. and Kania-Korwel et al.:[26, 27]

Rat liver microsomes from PB-pretreated rats were incubated with PCB 136 for 30 min.

&Data from Schnellmann et al.: Human liver microsomes were incubated with PCB 136 for 30 min.[25]

nd: not determined because 4–95 was not detected in the incubations.

-: not determined.